Quantum dynamics of impurities in a one-dimensional Bose gas

J. Catani,[1,2] G. Lamporesi,[1,2] D. Naik,[1] M. Gring,[3] M. Inguscio,[1,2] F. Minardi,[1,2,*] A. Kantian,[4] and T. Giamarchi[4]

[1]*LENS–European Laboratory for Non-Linear Spectroscopy and Dipartimento di Fisica, Università di Firenze, via N. Carrara 1,*
IT-50019 Sesto Fiorentino–Firenze, Italy
[2]*CNR-INO, via G. Sansone 1, IT-50019 Sesto Fiorentino–Firenze, Italy*
[3]*Vienna Center for Quantum Science and Technology, Atominstitut, TU-Wien, AT-1020 Vienna, Austria*
[4]*DPMC-MaNEP, University of Geneva, 24 Quai Ernest-Ansermet, CH-1211 Geneva, Switzerland*

Using a species-selective dipole potential, we create initially localized impurities and investigate their interactions with a majority species of bosonic atoms in a one-dimensional configuration during expansion. We find an interaction-dependent amplitude reduction of the oscillation of the impurities' size with no measurable frequency shift, and study it as a function of the interaction strength. We discuss possible theoretical interpretations of the data. We compare, in particular, with a polaronic mass shift model derived following Feynman variational approach.

I. INTRODUCTION

Low-dimensional and strongly interacting systems have sparked intense scientific interest in recent years in diverse research fields, such as solid-state physics, nanoscience, and atomic physics. In particular, strongly correlated systems display quantum phases dominated by quantum fluctuations, such as the Mott-insulator phase [1] and magneticlike ordered phases [2]. In low dimensions, the interplay between interactions among particles and confining potential can enhance the effect of quantum correlations, resulting in peculiar regimes, such as the Tonks-Girardeau or the sine-Gordon [3] regimes. Due to the unprecedented control over the interatomic interactions, the external trapping potentials, and the internal states of the atoms, ultracold atomic systems represent a versatile tool to explore these novel phenomena, and have already provided the way to realize some of these quantum phases [4]. A particular strength of cold atoms is the realization of systems that are hard to obtain in condensed-matter physics, such as multicomponent bosons of either different hyperfine states [5,6] or different species [7], as well as the study of real-time dynamics of quantum many-body systems.

In particular, cold atoms provide a way to realize a recently proposed new universal class of quantum systems, the so-called ferromagnetic liquids [8], occurring as the ground state of repulsively interacting two-component bosons. The time evolution of a spin flip, i.e., the excitation obtained by flipping one single bosonic "spin" from the fully spin-polarized ground state, thereby creating a localized "impurity," leads to a class of dynamics completely different to that of the standard (Luttinger-liquid) theory but possessing remarkable universal features [8–10]. The physics of such impurities propagating in a sea of the majority species is further connected to several longstanding questions in strongly correlated systems, both fermionic and bosonic. For fermionic systems and an immobile impurity, one example is the well-known x-ray edge problem, with the impurity leading to the Anderson orthogonality catastrophe [11]. The motion of the impurity then strongly affects this physics, as was probed both for impurities in ^{3}He [12] and, more recently, for minority species in interacting fermionic systems [13,14], in the context of Fermi-liquid theory. Inextricably linked to the study of the impurity motion is the notion of polarons [15], i.e., the occurrence of density fluctuations of the majority species, both for fermions and bosons, leading to renormalization of the impurity parameters, such as its mass. In one dimension, however, the nature of the bath is quite special, leading to the above-mentioned novel physical effects and, in particular, to subdiffusion at zero temperature. This problem is also directly related to the motion of a driven impurity which was investigated recently both theoretically [16–18] and experimentally [19]. A system where the impurity-bath interactions are adjustable over a wide range paves the way for the study of a wealth of physical phenomena.

In this work, we realize such a system using a species-selective dipole potential (SSDP) [20]. A minority species (K atoms) can diffuse into a majority species of (Rb) bosonic atoms, in a one-dimensional (1D) configuration (see Fig. 1). We study how the interspecies interactions reduce the oscillation amplitude of the impurities' size $\sigma(t) = \sqrt{\langle x^2 \rangle}$. We compare the data in the light of a model based on polaronic mass shifts.

The remainder of the paper is organized as follows: in Sec. II we describe the experimental procedure to prepare
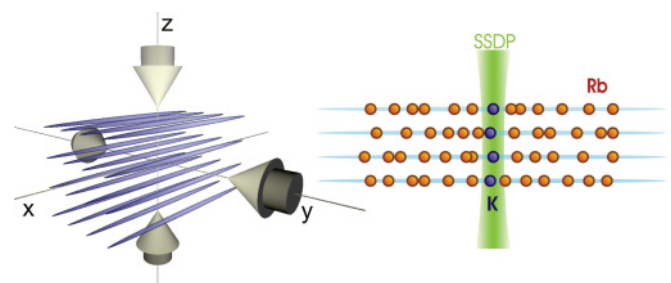

FIG. 1. (Color online) Ultracold Rb atoms with K impurities are loaded into an array of 1D systems, "tubes" (left). The SSDP light blade spatially localizes the impurities into the center of the Rb tubes (right).

*francesco.minardi@ino.it

the one-dimensional (1D) systems of K impurities initially localized in the surrounding Rb bath and measure their subsequent expansion; in Sec. III we report the experimental data; Sec. IV illustrates our theoretical model based on a quantum Langevin equation. By means of the Feynmann variational approach [21], we calculate the impurities' mass renormalization due to the interactions with the Rb bath. In Sec. V we compare the data with the results of the theoretical model, discussing the limitations and approximations involved. Finally, we summarize in Sec. VI.

II. EXPERIMENTAL PROCEDURE

The mixture of ^{87}Rb and ^{41}K is first cooled to 1.5 μK by microwave evaporation of Rb and sympathetic cooling of K in a magnetic trap, then loaded into a crossed dipole trap created by two orthogonal laser beams ($\lambda = 1064$ nm, waists $\simeq 70$ μm). Both species are spin polarized in their $|F = 1, m_F = 1\rangle$ hyperfine states, featuring magnetically tunable interspecies interactions in the 0–10 mT range. The mixture is further cooled by optical evaporation performed in a uniform magnetic field of 7.73 mT to adjust the interspecies scattering length a to the convenient value of 240 Bohr radii, ensuring both fast thermalization and a low rate of inelastic collisions.

At this point we set the magnetic field to 7.15 mT, corresponding to vanishing interspecies interactions, and we adiabatically raise a vertical (z) 1D optical lattice (waist 170 μm) to 15 (6.5) E_{rec} for Rb (K) in 200 ms. The lattice wavelength $\lambda = 1064$ nm results in a 2.3 times smaller lattice height for ^{41}K than for ^{87}Rb in units of the respective recoil energies ($E_{rec} = h^2/2m\lambda^2$). After adiabatic extinction of the dipole trap, both species move downward as collisions disrupt the gravity-induced Bloch oscillations [22] but, due to largely different tunneling times, K drops faster and, by adjusting the fall time, we reduce the gravitational sag between the two species in the dipole trap.

Subsequently, we further raise the vertical lattice to 60 E_{rec} for Rb and adiabatically switch on an additional standing wave with equal waist and strength along the y direction. Thus we create the array of 1D systems (tubes) by means of a two-dimensional (2D) lattice. The lattice transverse harmonic oscillator frequency, $\omega_\perp/2\pi = 34(45)$ kHz for Rb (K), exceeds both the temperature and the chemical potential, thus ensuring the 1D regime for both species.

The residual trapping frequency along the direction x of the tubes, 62 (87) Hz for Rb (K), is due to the inhomogeneous transverse profile of the lattice beams. An SSDP elliptic beam, orthogonal to the tubes, is then turned on in 50 ms, compressing K at the center of Rb and leaving the latter nearly unperturbed. This *light blade* has waists of 15 and 75 μm (x and z direction, respectively), wavelength of 770.4 nm, and power equal to 0.6 mW. Correspondingly, the depth and frequency are 11 μK and $\omega_K/(2\pi) = 1.0$ kHz.

Finally, the interaction strength $g_{1D,KRb}$ between K and Rb, is brought to the desired value by linearly ramping the magnetic field to its final value B_d. Instead, the interaction strength of the Rb atoms $g_{1D,Rb} = 2.36 \times 10^{-37}$ J m is independent of the applied magnetic field B_d.

The impurities' dynamics is initiated by rapidly extinguishing the light blade with a linear ramp of 0.5 ms.
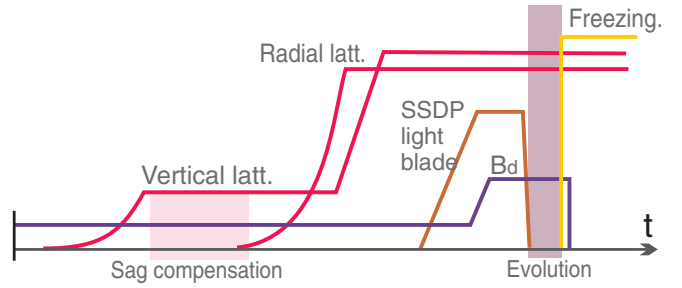

FIG. 2. (Color online) Time sequence of the experimental procedure used to prepare the K impurities in the middle of 1D tubes filled with Rb atoms.

Images of the impurities are taken once their motion has been frozen by suddenly adding a tight optical lattice along the tubes axis allowing for magnetic field to be extinguished in 15 ms and for atoms to be repumped in the hyperfine level suitable for imaging without significantly affecting their density distribution. The full experimental procedure is shown in Fig. 2.

Typically, we measure $(1.8 \pm 0.2) \times 10^5$ ^{87}Rb and $(6 \pm 2) \times 10^3$ ^{41}K atoms at 140 nK before loading the tubes. From the analysis of time-of-flight images, we obtain a temperature of the Rb sample in the 1D tubes of 350(50) nK. We estimate the Rb peak filling and density to be 180 atoms/tube and $n_{1D,Rb} \simeq 7\mu m^{-1}$, with a filling-averaged Lieb-Liniger parameter $(m_{Rb}g_{1D,Rb})/(\hbar^2 n_{1D,Rb}) \simeq 1$; the peak K filling is approximately 1.4 atoms/tube.

III. EXPERIMENTAL DATA

We record the oscillation of the impurities axial size $\sigma(t) = \sqrt{\langle x^2 \rangle}$ along the tubes as a function of time, through resonant *in situ* absorption imaging. We fit the absorption profiles by a two-dimensional Gaussian function. Figure 3 shows the evolution of the impurities axial size $\sigma(t)$ for four different values of the 1D interspecies interaction strength $g_{1D,KRb}$. Given the magnetic field B_d, hence the interspecies scattering length a [23], $g_{1D,KRb}$ is calculated following [24] and expressed in units of $g_{1D,Rb}$ as $g_{1D,KRb} = \eta g_{1D,Rb}$. We find the oscillation amplitude of $\sigma(t)$ to be large for $\eta \simeq 0$ (no interactions between impurities and 1D gas) and to decrease with η. Remarkably, for the largest oscillation strength, the impurities' oscillations are always confined inside the bath. In addition, we observe that, in addition to oscillating, $\sigma(t)$ increases linearly (at least initially) over time. In order to extract quantitative information, we fit the experimental data with a damped sine function with linear baseline: $\sigma(t) = \sigma_1 + \beta t - A e^{-\gamma \omega t} \cos[\sqrt{1 - \gamma^2}\omega(t - t_0)]$. Since in the following we will mainly focus on the oscillation amplitude, in Fig. 3 we show the fit parameters, $\omega/2\pi$, γ, and β.

We first notice that the oscillation frequency does not shift, within our error bars, with $g_{1D,KRb}$: such a surprising feature is further discussed below. Then we observe that, even in the absence of interactions at $\eta = 0$, a residual damping occurs, likely due to intraspecies collisions in tubes with more than one K atom. We also notice that, during the oscillations, the impurity cloud can grow larger than the Rb sample,
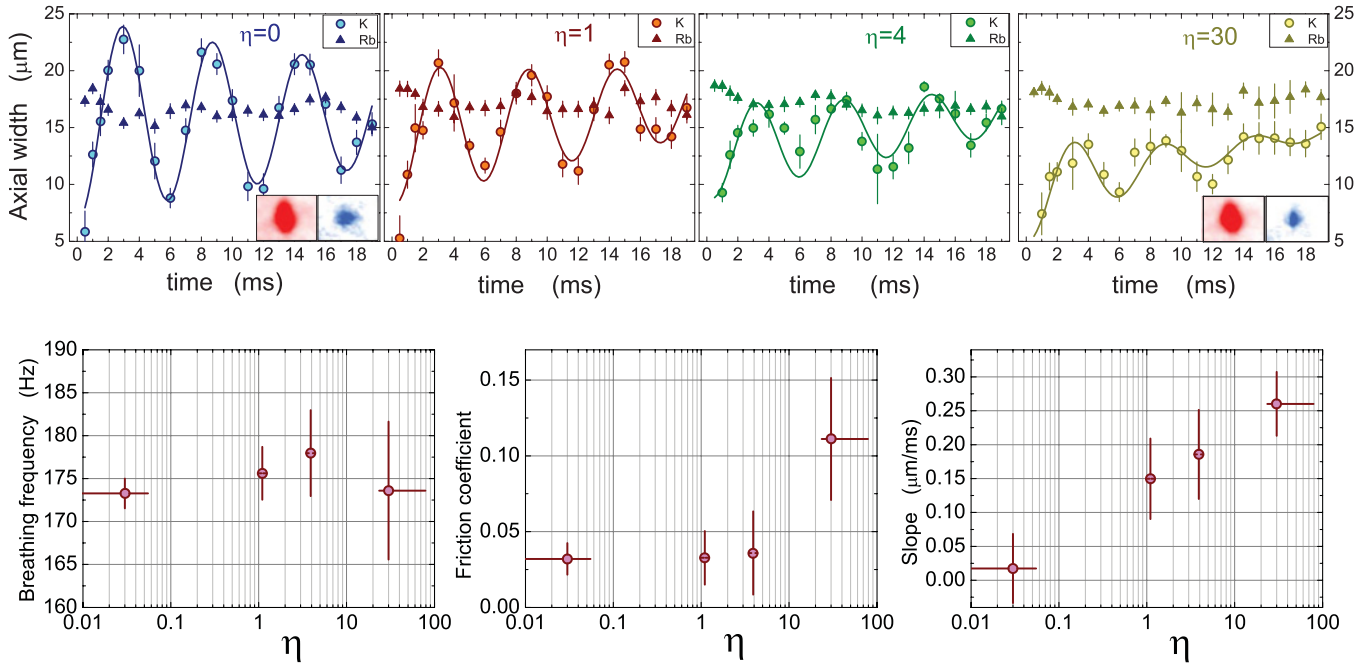
FIG. 3. (Color online) Upper panel: oscillations of the K impurities axial width $\sigma = \sqrt{\langle x^2 \rangle}$ after extinction of the confining SSDP, for different interaction strengths with the surrounding Rb bulk, $\eta = g_{1D,KRb}/g_{1D,Rb}$. Solid lines represent a fit to data, and triangles the Rb axial size. Inset images show the observed *in situ* density distributions of Rb (red, left) and K (blue, right) within a window of $200 \times 150 \,\mu$m. Lower panel: values of the fit parameters $\omega/2\pi$, γ, and β (left to right, see text for definition).

thus exploring the Rb inhomogeneous density profile. Such inhomogeneity along the tubes axis adds to the inhomogeneity of the tube's filling. In the following, we account for the inhomogeneity using the local density approximation, i.e., by considering homogeneous systems with different values of Rb linear density. As K impurities are initially confined in the middle of Rb, the first oscillation is less affected by Rb inhomogeneous density than the following ones. Therefore we focus our analysis on the value of the maximum size reached in the first oscillation, after 3 ms of expansion: $\sigma_p \equiv \sigma(t = 3\,\text{ms})$. Such value closely reflects the oscillation amplitude A as, for short times, both the slope and the damping have a negligible effect.

Figure 4 shows the dependence of σ_p on the relative coupling strength η: values of η of the order of the unity are sufficient to induce a significant amplitude reduction, if compared to the noninteracting case $\eta = 0$. It is important to remark that, if mean-field interactions dominated, we would observe an opposite behavior for positive and negative η values. As σ_p decreases with $|\eta|$, independently of its sign, we conclude that mere mean-field interactions cannot explain our experimental findings. We also notice a saturation behavior for $\eta > 4$ that cannot be due to the washing out of the Feshbach resonance caused by magnetic field instability ($\sim 10\mu$T). Instead, it might be related to a crossover to the three-dimensional (3D) regime, as we estimate that for $\eta = 15$ the mean-field interaction energy of the K impurities, $g_{1D,KRb}n_{1D,Rb}$, equals the band gap of the 2D lattice. As our theory cannot describe this 1D to 3D crossover, and furthermore the inclusion of the 1D bound states between K and Rb for $\eta < 0$ also cannot be adequately captured,

we have calculated $\sqrt{m_K/m_K^*}$ only in the range $0 < \eta \leqslant 8$ in Fig. 3.

To some extent, the amplitude of the first oscillation could reflect different preparation temperatures of the K sample in the light blade, as the efficiency of the thermalization with the Rb background depends on the strength of interactions. Thus, we recorded the first oscillation of K impurities prepared at large η and expanding at zero interactions, and compared it with the oscillations of samples prepared and expanded at large (or
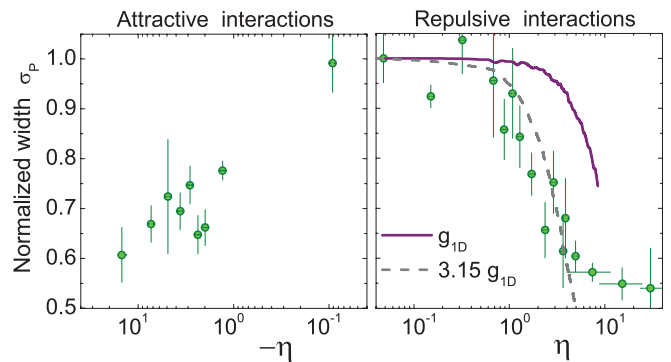

FIG. 4. (Color online) Experiment: impurities' axial size at the first oscillation maximum σ_p, normalized so that $\sigma_p = 1$ for $\eta = 0$, versus the coupling strength parameter $\eta = g_{1D,KRb}/g_{1D,Rb}$, for attractive (left, $\eta < 0$) and repulsive (right, $\eta > 0$) interactions (circles). Theory: $\sqrt{m_K/m_K^*}$ calculated with impurity-bath coupling $g_{1D,KRb}$ derived from two-body scattering [24] (solid line) and with $g_{1D,KRb}$ multiplied by a fit parameter (dashed line). Both curves are computed for a Rb density of 7 atoms/μm and $\tilde{\gamma} = 0$.
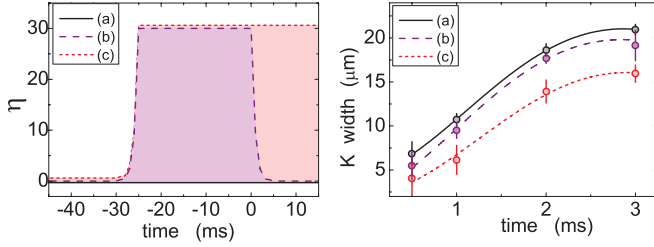
FIG. 5. (Color online) Amplitude of the first oscillation of the axial size of K impurities (right) following different preparation sequences (left): (a) η always negligible; (b) η large while K in the SSDP light blade and negligible during expansion at $t > 0$; and (c) η always large.

zero) interactions. We notice from Fig. 5 that the preparation has a nearly negligible impact on the oscillation amplitude, insufficient to explain the large differences observed between high and small η. Moreover, incomplete thermalization cannot explain why at large interactions σ_p lies below the Rb axial width, as shown in Fig. 3.

To summarize, the key experimental findings are (a) even for large η the oscillation frequency of $\sigma(t)$ does not deviate measurably from that of the noninteracting case (which is 2ω); (b) the larger $|\eta|$, the lower the amplitude of oscillation initially; (c) in the interacting case, besides oscillating, the impurities width increases over time in a seemingly linear fashion; and (d) at long times $\sigma(t)$ equilibrates to about the same value, independently of η.

IV. THEORETICAL MODEL

A complete explanation of the observed phenomena is an interesting and open problem. Motivated by the observed shape of $\sigma(t)$, we give here a semiempirical analysis of the oscillation through the model of a damped, quantum harmonic oscillator in contact with a thermal bath, i.e., a quantum Langevin equation [25], $\dot{\hat{x}}(t) = \hat{p}(t)/m_K^*$, $\dot{\hat{p}}(t) = -k^*\hat{x}(t) - \tilde{\gamma}\hat{p}(t) + \hat{\xi}(t)$, as a framework to order and provide a first interpretation of the findings. Here, $\hat{x}(t)$ and $\hat{p}(t)$ are, respectively, the position and momentum operators of one ^{41}K atom whose mass m_K^* and spring constant k^* are renormalized by interactions with the bath. In addition to the exponential damping $-\tilde{\gamma}\hat{p}(t)$, we account for the fluctuations of the bath by the noise operator $\hat{\xi}(t)$, whose correlator $\langle\hat{\xi}(t)\hat{\xi}(t')\rangle \propto \tilde{\gamma}$ is approximated by using the thermal quantum statistics of a set of harmonic oscillators at constant spectral density [25]. The operator $\hat{\xi}(t)$ causes the gradual increase of the impurities' width, corresponding to heating from the thermal component of the bath.

Various effects could account for the change of amplitude. A dominant mean-field interaction for $\eta > 0$ would make the effective potential for the K shallower, resulting in σ_p *increasing* with η, at odds with observed behavior. Another possibility is the damping from the $\tilde{\gamma}$ term. However, this is also inconsistent with the observed data: within the quantum Langevin approximation, and at the experimental temperatures, any but very small values of $\tilde{\gamma}$ result in strong heating contributions from the correlator $\langle\hat{\xi}(t)\hat{\xi}(t')\rangle$, such that overall σ_p increases with η.

At variance with the two above-mentioned effects, a mass renormalization of the K impurities due to polaronic effects [21] is a very good starting point to explain the decrease of σ_p.

A. Polaronic mass shift

We calculate the mass shift $M = m_K^* - m_K$ using Feynman's variational theory for the polaron [21]. Taking the combined impurity-bath Hamiltonian

$$\hat{H} = \frac{\hat{p}^2}{2m_K} + \sum_{k \neq 0} \epsilon_k \hat{b}_k^\dagger \hat{b}_k + \sum_{k \neq 0} V_k e^{ik\hat{x}}(b_k + b_{-k}^\dagger), \quad (1)$$

where the Rb bath has been approximated as a Tomonaga-Luttinger liquid with linearized density fluctuations around a homogeneous background density, described by the bosonic operators $\hat{b}_k, \hat{b}_k^\dagger$ with $\epsilon_k = v_s|k|$, $V_k = g_{1D,KRb}(K|k|/2\pi L)^{1/2}e^{-|k|/2k_c}$, and where v_s is the sound velocity of Rb, K the Luttinger parameter, related to the effective Rb-Rb interaction, and k_c the cutoff momentum. These quantities can be related to a homogeneous 1D Rb gas with arbitrary contact interactions [26]; as a working theory for inhomogeneous 1D systems is difficult to obtain, we use this homogeneous theory instead, evaluating it for different Rb densities in the center of the trap. We find that the results are not that strongly depending on the precise value of the Rb density.

Evaluating the full partition function $Z = \text{Tr}(e^{-\beta\hat{H}})$ as a path integral and integrating out the Rb bath yields an action S for the K atom that is nonlocal in time:

$$S = \int_0^{\beta\hbar} d\tau \frac{m_K}{2}\dot{x}^2(\tau) - \sum_k \frac{V_k^2}{2\hbar} \int_0^{\beta\hbar} d\tau$$

$$\times \int_0^{\beta\hbar} d\tau' \, G(k, |\tau - \tau'|)e^{ik[x(\tau)-x(\tau')]}, \quad (2)$$

where $G(u,k) = \cosh[\epsilon_k(u - \hbar\beta/2)]/\sinh(\hbar\beta\epsilon_k/2)$. The mass shift enters through the Feynman trial action S_0,

$$S_0 = \int_0^{\beta\hbar} d\tau \frac{m_K}{2}\dot{x}^2(\tau) + \frac{MW^3}{8} \int\int_0^{\beta\hbar}$$

$$\times d\tau \, d\tau' \frac{\cosh(W|\tau - \tau'| - W\hbar\beta/2)}{\sinh(W\beta\hbar/2)}[x(\tau) - x(\tau')]^2,$$

which depends on two parameters, the mass shift M and W, which are chosen by minimizing the trial free energy $F_0 + \langle S - S_0\rangle/(\hbar\beta) \geq F = -(1/\beta)\ln Z$.

The explicit expression of the trial free energy is

$$F_0 + \frac{1}{\beta\hbar}\langle S - S_0\rangle$$

$$= \ln\left[\sinh\left(\frac{\beta\hbar W\alpha}{2}\right)\right] - \ln\left[\sinh\left(\frac{\beta\hbar W}{2}\right)\right] - \ln\alpha$$

$$- \frac{M}{2(m_K + M)}\left[\frac{\hbar\beta W\alpha}{2}\coth\left(\frac{\beta\hbar W\alpha}{2}\right) - 1\right]$$

$$- \sum_k \frac{V_k^2}{\hbar} \int_0^{\hbar\beta} du\left(1 + \frac{u}{\hbar\beta}\right)G(k,u)\mathcal{K}(k,u), \quad (3)$$
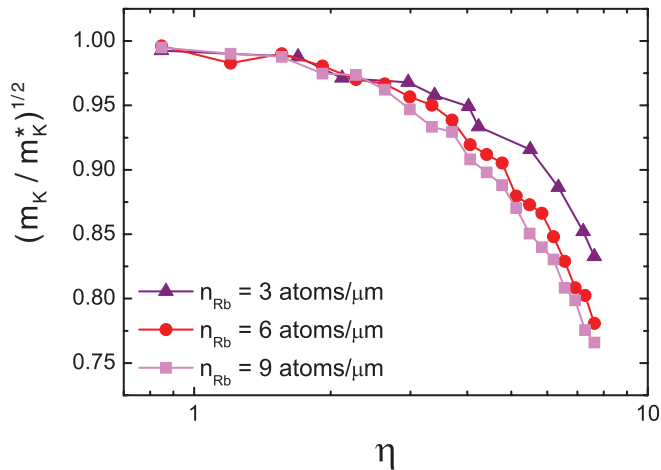
FIG. 6. (Color online) Square root of the inverse impurities' renormalized mass versus interspecies interaction strength η, calculated for different values of Rb density. This quantity directly compares with the measured K width σ_p.

where $\alpha = \sqrt{1 + M/m_K}$, and

$$\mathcal{K} = \exp\left[-\frac{\hbar k^2}{2(m_K + M)}\left(u - \frac{u^2}{\hbar\beta} + \frac{M}{m_K}\right.\right.$$
$$\left.\left. \times \frac{\cosh(W\alpha\hbar\beta/2) - \cosh[W\alpha(\hbar\beta/2 - u)]}{W\alpha\,\sinh(\hbar\beta W\alpha/2)}\right)\right]. \quad (4)$$

which we then minimize numerically to obtain the mass shift M.

We apply this theory to an experiment with an inhomogeneous density distribution of bath particles (due to the external confinement of the Rb atoms). For this approach to be reasonable, the mass shift should not depend too strongly on a shift in Rb density, which Fig. 6 shows to be indeed the case (all other parameters are as in the experiment).

Note that one can easily add a term corresponding to a parabolic confining potential in the action (2) and repeat the variational procedure to find the effective mass. Quite intuitively, one finds that the tighter the confinement, the smaller is the mass renormalization. This strongly suggests that before the blade is released one should consider that the K impurity has its bare mass. This is clearly a point that would need to be more quantitatively tested by, e.g., a Monte Carlo calculation.

V. COMPARISON OF DATA AND THEORY

Strongly simplifying the bath (see [25]) for a small $\tilde{\gamma}$—as the data suggest—we obtain the functional form for $\sigma(t)$ used to fit the oscillations in Fig. 3. The theoretically predicted σ_p is proportional to $1/\sqrt{m_K^*}$. Therefore, in Fig. 4 we compare the measured σ_p normalized to the value at zero interactions to the calculated values of $\sqrt{m_K/m_K^*}$: the theoretical curve reproduces the experimental trend and magnitude of the amplitude reduction fairly well.

As the variational approach cannot take the inhomogeneity of the bath into account, we approximate the translationally invariant theory with representative values for the Rb density

in the center of the trap. We find that, in the parameter range of the experiment, the mass shift is rather insensitive to the Rb density.

We also considered the possibility that $g_{1D,KRb}$ in the experiment (i.e., at finite density) may be different from the one obtained in the standard 1D two-body scattering theory [24,27]. While those formulas have indeed been demonstrated to well describe the position of the confined-induced resonances (CIR) also in the regime of finite density, it is currently unknown how accurate it is for the actual value of $g_{1D,KRb}$ away from the CIR. We find that a least-square fit of the theory to data with a value of $3.15g_{1D,KRb}$ fits the experiment better.

Concerning the mass shift theory for σ_p, we must note that for the trap parameters and temperatures it relies on the assumption that the mass of K is not or is only insignificantly renormalized inside the light blade during preparation. This is supported by calculations of the mass renormalization that include a parabolic trap for the K, which show the mass shift becoming smaller, the deeper the trap, eventually becoming zero. This simple extension of Feynman's approach is, however, ill suited to quantitative calculations of concrete values of the mass shift in a tight confinement, and we therefore must leave the quantitative test of this assumption to strong numerical methods.

The above interpretation based on the polaronic mass shift also predicts an increase of the oscillation period, which for large η would be beyond the 5% experimental error bars. To reconcile this apparent contradiction with the data, we need to consider the physical processes resulting in an effective upward renormalization of the spring constant k^*. Such processes are more easily visualized in the limit of impenetrability: when the impurities cannot get across the bath atoms, their displacement from the trap bottom costs the additional harmonic potential energy of the bath atoms moving uphill. While this is observed in proof-of-principle simulations for simplified models, quantitatively estimating the value of k^* is difficult with current methods and will require further, more refined analysis.

VI. CONCLUSIONS

In conclusion, we have investigated the dynamics of impurities in 1D atomic samples as we varied their interaction strength with the surrounding bath of weakly interacting bosons by more than two orders of magnitude. We observe the amplitude of the impurities' quadrupole oscillations decreasing with the absolute value of the interaction strength, a fact unexplained by mere mean-field interactions. An analysis of the data in the light of a simplified quantum Langevin equation suggests that polaronic mass shift plays a role in the amplitude reduction.

[1] M. Imada, A. Fujimori, and Y. Tokura, Rev. Mod. Phys. **70**, 1039 (1998).

[2] A. Auerbach, *Interacting Electrons and Quantum Magnetism* (Springer, Berlin, 1998).

[3] T. Giamarchi, in *Quantum Physics in One Dimension*, International Series of Monographs on Physics, Vol. 121 (Oxford University Press, Oxford, UK, 2004).

[4] I. Bloch, J. Dalibard, and W. Zwerger, Rev. Mod. Phys. **80**, 885 (2008).

[5] C. J. Myatt, E. A. Burt, R. W. Ghrist, E. A. Cornell, and C. E. Wieman, Phys. Rev. Lett. **78**, 586 (1997).

[6] J. Stenger, S. Inouye, D. M. Stamper-Kurn, H.-J. Miesner, A. P. Chikkatur, and W. Ketterle, Nature (London) **396**, 345 (1998).

[7] G. Modugno, M. Modugno, F. Riboli, G. Roati, and M. Inguscio, Phys. Rev. Lett. **89**, 190404 (2002).

[8] M. B. Zvonarev, V. V. Cheianov, and T. Giamarchi, Phys. Rev. Lett. **99**, 240404 (2007).

[9] A. Imambekov and L. I. Glazman, Phys. Rev. Lett. **100**, 206805 (2008).

[10] M. B. Zvonarev, V. V. Cheianov, and T. Giamarchi, Phys. Rev. B **80**, 201102 (2009).

[11] G. D. Mahan, *Many Particle Physics* (Springer, New York, 2007).

[12] A. Rosch and T. Kopp, Phys. Rev. Lett. **75**, 1988 (1995), and references therein.

[13] A. Schirotzek, C.-H. Wu, A. Sommer, and M. W. Zwierlein, Phys. Rev. Lett. **102**, 230402 (2009).

[14] S. Nascimbène, N. Navon, K. J. Jiang, L. Tarruell, M. Teichmann, J. McKeever, F. Chevy, and C. Salomon, Phys. Rev. Lett. **103**, 170402 (2009).

[15] R. P. Feynman, *Statistical Mechanics* (Benjamin Reading, MA, 1972).

[16] G. E. Astrakharchik and L. P. Pitaevskii, Phys. Rev. A **70**, 013608 (2004).

[17] A. Y. Cherny, J.-S. Caux, and J. Brand, Phys. Rev. A **80**, 043604 (2009).

[18] D. M. Gangardt and A. Kamenev, Phys. Rev. Lett. **102**, 070402 (2009).

[19] S. Palzer, C. Zipkes, C. Sias, and M. Köhl, Phys. Rev. Lett. **103**, 150601 (2009).

[20] J. Catani, G. Barontini, G. Lamporesi, F. Rabatti, G. Thalhammer, F. Minardi, S. Stringari, and M. Inguscio, Phys. Rev. Lett. **103**, 140401 (2009).

[21] R. P. Feynman, Phys. Rev. **97**, 660 (1955).

[22] H. Ott, E. de Mirandes, F. Ferlaino, G. Roati, G. Modugno, and M. Inguscio, Phys. Rev. Lett. **92**, 160601 (2004).

[23] G. Thalhammer, G. Barontini, L. De Sarlo, J. Catani, F. Minardi, and M. Inguscio, Phys. Rev. Lett. **100**, 210402 (2008).

[24] V. Peano, M. Thorwart, C. Mora, and R. Egger, New J. Phys. **7**, 192 (2005).

[25] P. Z. C. W. Gardiner, *Quantum Noise*, 3rd ed. (Springer, New York, 2004).

[26] M. A. Cazalilla, R. Citro, T. Giamarchi, E. Orignac, and M. Rigol, Rev. Mod. Phys. **83**, 1405 (2011).

[27] M. Olshanii, Phys. Rev. Lett. **81**, 938 (1998).